Article

Microstructural Analysis and Mechanical Characterization of Shape Memory Alloy Ni-Ti-Ag Synthesized by Casting Route

Khansaa Dawood Salman [1], Wisam Abed Kattea Al-Maliki [2,3], Falah Alobaid [2,*] and Bernd Epple [2]

1 Department of Electromechanical Engineering, University of Technology, Baghdad 19006, Iraq; 50123@uotechnology.edu.iq

2 TU Darmstadt, Institut Energiesysteme und Energietechnik, Otto-Berndt-Straße 2, 64287 Darmstadt, Germany; wisam.a.kattea@uotechnology.edu.iq (W.A.K.A.-M.); bernd.epple@est.tu-darmstadt.de (B.E.)

3 Mechanical Engineering Department, University of Technology, Baghdad 19006, Iraq

* Correspondence: falah.alobaid@est.tu-darmstadt.de; Tel.: +49-61-5116-6691; Fax: +49-61-5116-5685

Abstract: The purpose of the current research is to study the microstructure and mechanical properties of Ni-Ti-Ag shape memory alloys prepared by the casting route. Ag (grain size at 1 mm) was incorporated into Ni-Ti alloys at varying percentages of weight (0, 1.5, 3 and 4.5 wt.% Ag) to produce shape memory alloys using a Vacuum Arc Re-melting (VAR) furnace. Microstructural analysis was defined by FESEM microscopy and XRD examinations, while the transformation temperatures of the Ni-Ti-Ag shape memory alloy were determined by DSC examination. On the other hand, determination of mechanical properties was carried out using micro-hardness and compressive tests. The results of this work show that Ag was dispersed homogeneously into the Ni-Ti alloy. Moreover, two primary phases (austenite phase and martensite phase) emerged with few impurities. The results of the XRD examination show that the number of Ag peaks increased with the increase in weight percentage of Ag. The transformation temperature of the austenitic phase was defined as -1.6 °C by DSC. The mechanical characterizations increased with the increase in weight percentages of Ag (1.5, 3 and 4.5 wt.%), and significantly affected the mechanical properties of the Ni-Ti alloy. An improvement in compressive strength (42.478%) was found for the alloy with 3 wt.% Ag, while the micro-hardness results show a slight decrease in micro-hardness (8.858%) for the alloy with 4.5 wt.% Ag.

Keywords: shape memory alloys; Ni-Ti-Ag; casting; VAR furnace; microstructure; XRD; mechanical properties

1. Introduction

Shape memory alloys (SMAs) are the main classification of smart alloys owing to their unique properties. Smart materials are metallic alloys that respond to mechanical stresses and temperature, creating internal deformation of about 2–10%. Smart alloys are considered thermo-mechanical materials used in many mechanical applications due to their ability to return (remember) to their shape after the removal of external loads [1]. The shape memory effect is created when the SMAs undergo applied stresses at a constant temperature, while super elasticity is created at a temperature higher than the austenite finish temperature (Af) and constant stress; hence, the SMAs return to their original shape after removing the load. Ni-Ti alloys (Nitinol) are important shape memory alloys that consist of two main phases; the first phase is austenite (B2) and the second phase is martensite (B19). The austenite phase is created at a high temperature and transforms into the martensite phase at a low temperature. Phase transformation from the austenite phase to the martensite phase is affected by many factors such as the heating–cooling cycle, Ni concentration, and the processing conditions when using the casting route [2]. Shape memory alloys are commonly used in mechanical and biological applications that require smart alloys due to their unique properties, such as recovery to their original shape, with a large amount of

deformations. Each one of these properties consists of two-phase transformations: the first is the martensite phase, which occurs at high pressure and low temperature (Mf), and the second is the austenite phase, which occurs at low pressure and high temperature (Af). For a specific temperature that is lower than the transformation temperature, the martensite phase was created (twin) as a soft phase and was deformed by (de-twinning). Many metal alloys tend to draw back to their original shape when heated above the transformation temperature; however, increasing the applied stress can create plastic deformation. Many metallic alloys have a recovery of about 0.1%, while the SMAs have a recovery of about 7–8% [1,3].

Generally, there are two techniques used to fabricate SMAs: powder metallurgy or the casting method, which are classified as vacuum induction melting (VIM), electron beam melting (EBM) and vacuum arc re-melting (VAR). The preferred technique is vacuum arc re-melting (VAR) as it offers a high purity shape memory alloy, especially Ni-Ti-Ag. On the other hand, Ni-Ti based SMAs are not suitable for many purposes; therefore, to improve the properties of Ni-Ti SMAs, various elements have been added such as Fe, Co and V, which are used to decrease the transformation temperature. Au, Zr, Pt and Hf are used to raise the transformation temperature, and Cu is used to decrease the hysteresis loop, especially when adding Fe and Nb [2]. Ag is an important element due to its superior and anti-bacterial material and its stability. Hence, Ag is considered the best element incorporated into Ni-Ti-based alloys to produce Ni-Ti-Ag composite material with higher strength compared with Ni-Ti-based alloys and higher anti-bacterial activity [4–11]. The main manufacturing processes used to produce SMAs are the casting method and powder metallurgy method, followed by heat treatment to minimize the internal stresses and improve the properties of the manufactured SMAs [12]. The aim of this work is to synthesize Ni-Ti-Ag SMAs by the casting method using a VAR furnace and to study the effect of the addition of Ag on the microstructure and mechanical properties of SMAs.

2. Experimental Procedures

In the present work, commercially pure Ni, Ti and Ag were used with the composition of Ni (50) wt.% with Ti (50, 48.5, 47, 45.5) wt.% and Ag (0, 1.5, 3, 4.5) wt.%. Ni-Ti-Ag shape memory alloys were synthesized by the casting route using a vacuum arc re-melting (VAR) furnace. The arc-melting process was carried out in an inert Ar atmosphere (99.99 vol.% purity) at approximately 500 mbar pressure. Prior to arc melting, a vacuum was applied to a bell jar at a double pressure of about 5×10^{-4} mbar, followed by refilling with argon gas. To improve the mixing process, it was necessary to turn the button over after each arc melting stage and repeat it until the arc-melting process was complete. After repeating the arc-melting process four times, samples with dimensions of about (10 cm $\times$ 2.5 cm $\times$ 1 cm) inside the furnace tube were homogenized in accordance with the heating cycle under an Ar gas atmosphere. Fast heating was carried out at 600 °C using about 15 °C/min heating rate, which was subsequently followed by heat treatment at a slow warming level of 600–1000 °C, using about 15 °C/min heating rate maintained at 1000 °C for 8 h, followed by rinsing with water.

3. Characterization

X-ray diffraction (XRD) patterns were used to identify each phase, using the X-ray diffractometer model (Panalytical X'pert) with CuKα radiation at λ = 1.5405 A° at an ambient temperature. The microstructure of Ni-Ti-Ag samples was analysed on a Field Emission Scanning Electron Microscopy (FESEM) model (ZEISS SIGMA VP), which was used to describe the surface morphology characteristics. The phase transformation behaviour of the experimental samples was investigated by differential scanning calorimetry (DSC), using a (NETZSCH DSC 214 Polyma) calorimeter with a heating rate of about 10°/min. The mechanical properties and stress–strain curves of the Ti-Ni-Ag alloys were studied in compression testing. Compression testing was carried out by (STM-50), a universal testing machine with a 5 mm/min testing speed. Micro-hardness testing of the samples

was carried out by Vickers apparatus (Diamond pyramid) according to ASTM E92 standard, and Force applied (Kgf): 10 HV with Duration of force: 10–15 s.

4. Results

4.1. Microstructure Analysis

The microstructure of the shape memory alloys, which contain different wt.% of Ag particles, was achieved using FESEM testing, as shown in Figure 1A–D. The photomicrographs reveal the homogeneous dispersion of Ag particles in the Ni-Ti alloys with observed voids. Particles of Ag were melted and filled the interstitial voids between the Ni-Ti alloy elements, owing to the low melting point for Ag. Parallel lines can be seen in the FESEM photomicrographs of the homogenized alloys in Figure 1C,D. These lines are considered the martensite phase (B19′), formed as a result of the thermal transformation of austenitic (B2) Ni-Ti shape memory alloys. This first-order phase transformation provides SMAs with the ability to recover their unique shape [13].
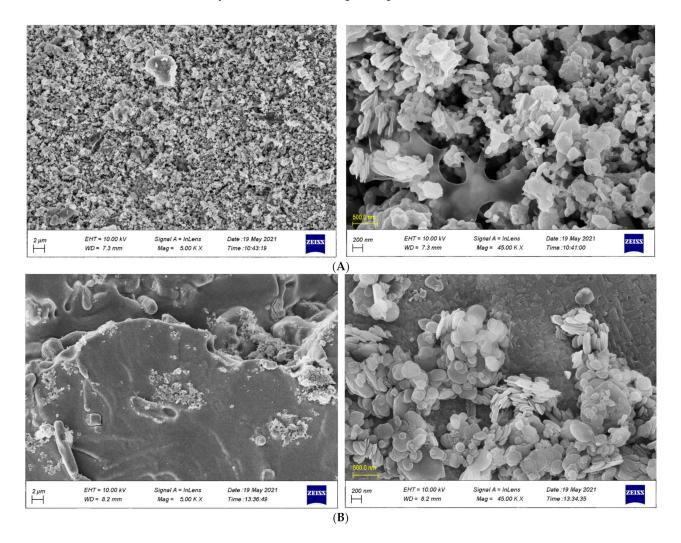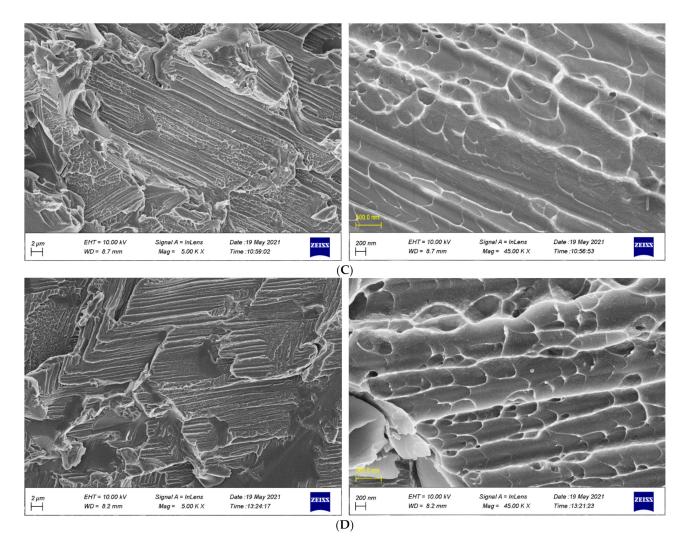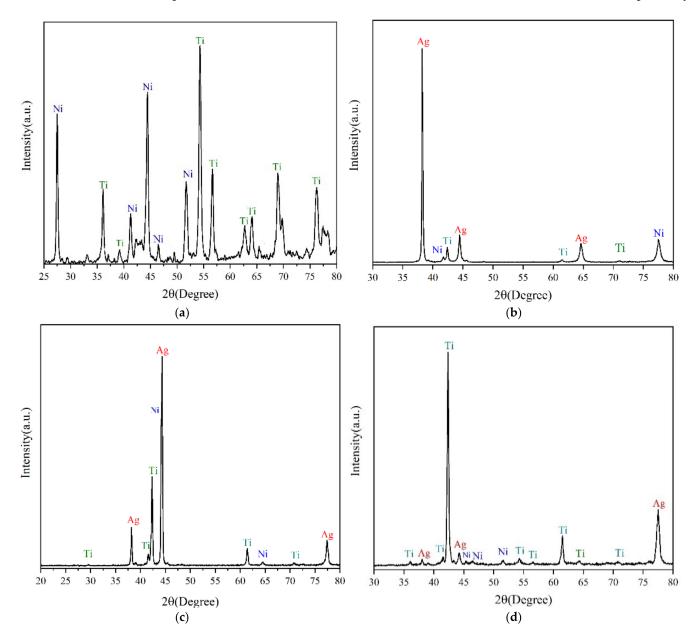

(A)

(B)

Figure 1. *Cont.*

Figure 1. (**A**): 0 wt.% Ag; (**B**) 1.5 wt.% Ag; (**C**) 3 wt.% Ag; (**D**) 4.5 wt.% Ag.

4.2. XRD Results

Figure 2a reveals XRD peaks of the Ni-Ti shape memory alloy (0 wt.% Ag) calculated at room temperature with a diffraction angle (2θ) varying about 25–80°. The strongest peaks for the Ti phase formed at (2θ): 36.12°, 39.24°, 54.35°, 56.7°, 62.77°, 64.12°, 68.9° and 76.4°, respectively, for hkl (100), (101), (102), (200), (110), (211), (103) and (112). While the Ni phase was created at (2θ): 27.47°, 41.38°, 44.47°, 46.54° and 51.74° for hkl (101), (002), (111), (011) and (200), respectively. This is owed to the formation of Ti2Ni (Austenite phase) and M or Ti002 (martensite phase). Figure 2b reveals XRD peaks for the Ni-Ti shape memory alloy for (1.5 wt.% Ag); this created three principal phases: Ni, Ti and Ag phases, which appear at (2θ), varying between 30 and 80°. The Ti phase was created at (2θ): 42.51°, 61.5° and 71.0° for hkl (101), (110) and (103), respectively. In addition, the Ni phase was generated at (2θ) at around 41.8° and 77.5° for the planes (111) and (220), respectively. The addition of element (Ag) was generated at (2θ): 38.26°, 44.45°, and 64.58° for hkl (111), (220) and (311), respectively, while Figure 2c reveals the XRD peaks for the Ni-Ti shape memory alloy for (3 wt.% Ag), producing three major phases: Ni, Ti and Ag phases at (2θ), varying between 30 and 80°. The Ti phase was created at (2θ): 29.57°, 41.57°, 42.32°, 61.43° and 70.84° for hkl (100), (002), (101), (102) and (103), respectively, while the Ni phase formed at (2θ): 44.17° and 64.53° for hkl (011) and (220). The Ag phase formed at (2θ): 38.24°, 44.35° and 77.4° for hkl (111), (200) and (311), respectively. Finally, Figure 2d reveals the XRD peaks for the Ni-Ti shape memory alloy with (4.5 wt.% Ag). Three principal phases were formed: Ni, Ti and Ag phases. Together, these phases formed at (2θ) in the range of 30–80°. The Ti
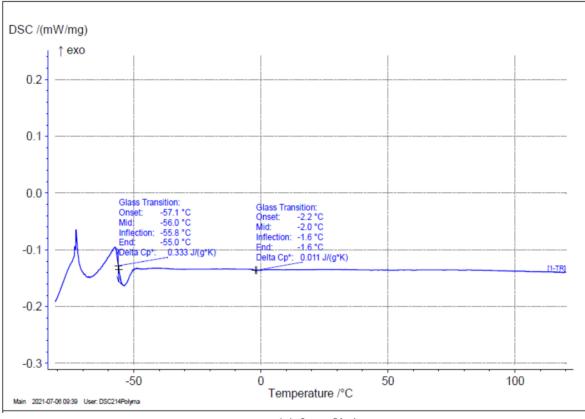
phase was created at (2θ): 25.29°, 41.43°, 42.35°, 54.3°, 56.53°, 61.53°, 64.38° and 70.85° for hkl (100), (002), (101), (102), (200), (110), (211) and (103), respectively, while the Ni phase formed at (2θ): 46.4°, 46.53° and 51.55° for hkl (111), (011) and (200), respectively. The Ag phase formed at (2θ): 27.38°, 44.23° and 77.53° for hkl (111), (220) and (311), respectively.
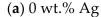

Figure 2. X-ray diffraction patterns for, (**a**): Ni-Ti, (**b**): Ni-Ti-Ag 1.5 wt.%, (**c**): Ni-Ti-Ag 3 wt.% and (**d**): Ni-Ti-Ag 4.5 wt.%.

4.3. DSC Results

Figure 3a–d shows the transformation temperatures for the alloys for all the specimens of shape memory alloys, with and without adding Ag. The transformation temperature was measured as the intersection of the two tangential lines of the curves. Ni-Ti was indicated at the austenitic transformation initial temperature of around −1.6 °C, and for the Ni-Ti-Ag alloys at about 19.7 °C, 12.7 °C and 12.3 °C, for Ag contents of 1.5, 3 and 4.5 wt.%. It should be mentioned here that the specific heat of Ni-Ti-Ag alloy (Cp*) is variable. The Ni-Ti-Ag alloys showed higher transformation temperatures compared with Ni-Ti-based alloys. In spite of the transformation temperatures of the Ni-Ti-Ag alloys, a slight decrease was observed with the rising weight percentages of Ag.
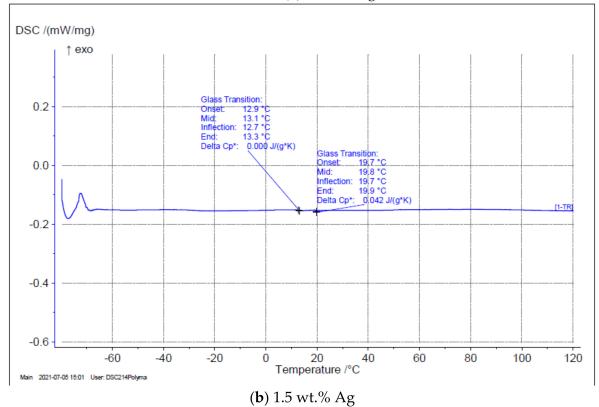
(**a**) 0 wt.% Ag

(**b**) 1.5 wt.% Ag

Figure 3. *Cont.*

(**c**) 3 wt.% Ag
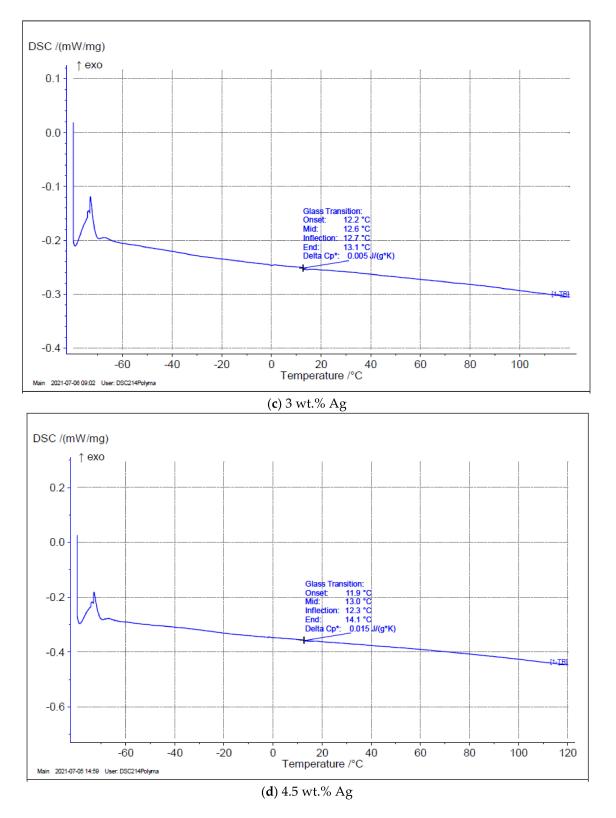

(**d**) 4.5 wt.% Ag

Figure 3. The DSC curves of Ni-Ti-Ag alloys.

4.4. Compression Results

Figure 4 shows the mechanical characteristics of the Ti-Ni matrix alloys for various wt.% of Ag during compression testing at room temperature. Compression testing showed that B2→R→B19′ martensite transformation was carried out by the deformation that occurs in all alloys before fracture. According to the stress–strain behaviour, the deformation

process of Ti-Ni-Ag alloys can be divided into three stages. The first phase, B2, is characterized by the initial linear fraction and strain accumulation due to elastic deformation of the martensite phase. The martensitic second phase R appears in the presence of the stress plateau, which indicates that the martensite transformation process occurred. In the third stage of deformation, the martensite phase, B19, can be seen, owing to the permanent deformation of this phase [14,15]. Moreover, the crystal structure of Ag was FCC, therefore, with increasing the wt.% of Ag incorporated into the Ni-Ti matrix, the volume fraction increased. Afterwards, Ag particles caused internal stresses in the Ni-Ti matrix through the deformation process and made the alloy brittle. The homogeneity dispersion of nanoparticles with a significant volume fraction of reinforcing material into Ti-Ni resulted in the high strength of the Ti-Ni alloy incorporated with 3 wt.% Ag. Additionally, the increment in densities of grain boundaries created the homogeneity of plastic strain in the matrix and then increased the volume; the level of internal stresses then decreased [15].
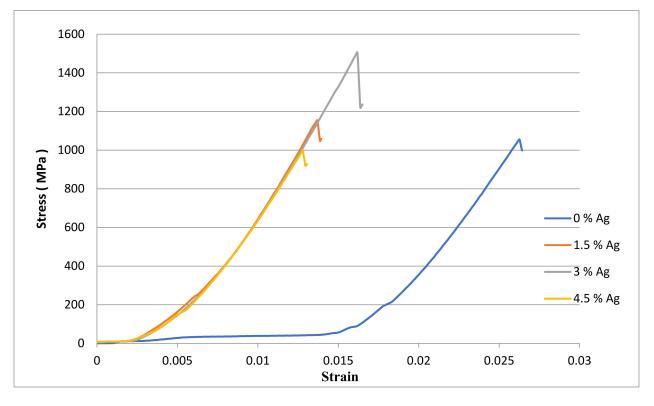

Figure 4. Compressive stress–strain curves of the Ni-Ti-Ag samples.

4.5. Micro-Hardness Results

Figure 5 and Table 1 show the values of the micro-hardness (Vickers Hardness) for the Ni-Ti-Ag SMAs with different weight percentages of Ag. For each sample, four readings were taken and then their average value was calculated. The results of this test showed a slight decrease in micro-hardness with the increase in weight percentages of Ag. The decrease in micro-hardness of the Ni-Ti-Ag SMAs was due to the ductility of silver and its lower scratching resistance than the Ni-Ti matrix.
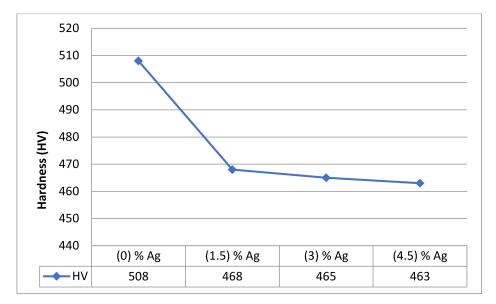
Figure 5. Micro-hardness (Hv) of Ti-Ni-Ag alloys.

Table 1. Compressive stress and microhardness results.

Test \ Sample	0% Ag	1.5% Ag	3% Ag	4.5% Ag
Compression stress (MPa)	1055	1155	1507	1000
Hardness (HV)	508	468	465	463

5. Conclusions

Ni-Ti-Ag shape memory alloys have been successfully synthesized by the casting technique using a VAR furnace. Ag, as an additive material, was incorporated into Ni-Ti based alloys at different weight percentages (1.5, 3 and 4.5 wt.%). The result of the FESEM analysis showed that Ag homogeneously dispersed into the Ni-Ti-based alloy, creating two main phases (austenite and martensite). While XRD analysis demonstrated the emergence of the main phases: Ni, Ti and Ag, as evidenced in the XRD peaks. In addition, the increase in weight percentage of Ag led to an increase in Ag peaks. DSC examination demonstrated that the austenite transformation starting temperature at (-1.6 °C) and transformation temperatures with increasing Ag wt.% are 19.7 °C, 12.7 °C and 12.3 °C, respectively. The addition of Ag significantly affected the mechanical properties of the Ni-Ti-based alloy in regard to its micro-hardness and compressive strength. The maximum value of compressive strength was obtained in the alloy with 3 wt.% Ag, while the results of micro-hardness testing showed a slight decrease with the increase in weight percentage of Ag.

References

1. Riad, A.; Ben Zohra, M.; Mansouri, M.; Alhamany, A. The shape memory alloy controlled by the sun's radiation effect. *J. Comput. Methods Sci. Eng.* **2018**, *18*, 117–127. [CrossRef]
2. Wang, J.; Moumni, Z.; Zhang, W.; Zaki, W. A thermomechanically coupled finite deformation constitutive model for shape memory alloys based on Hencky strain. *Int. J. Eng. Sci.* **2017**, *117*, 51–77. [CrossRef]
3. Vyavahare, P.V.; Karthikeyan, C.P. Shape memory effect and performance of a nitinol engine. *Aust. J. Eng. Technol. Res.* **2017**, *2*, 109–119.
4. Wahhab, H.A.A.; Al-Maliki, W.A.K. Application of a Solar Chimney Power Plant to Electrical Generation in Covered Agri-cultural Fields. In *IOP Conference Series: Materials Science and Engineering*; IOP Publishing: Kerbala, Iraq, 2020; p. 012137.
5. Al-Maliki, W.; Mahmoud, N.; Al-Khafaji, H.; Alobaid, F.; Epple, B. Design and Implementation of the Solar Field and Thermal Storage System Controllers for a Parabolic Trough Solar Power Plant. *Appl. Sci.* **2021**, *11*, 6155. [CrossRef]
6. Sanaani, Y.T.; Alshorman, A.; Alshurman, K. A Novel Design of Flexure Based, Shape Memory Alloy Actuated Microgripper. In Proceedings of the ASME International Mechanical Engineering Congress and Exposition, Tampa, FL, USA, 3–9 November 2017; American Society of Mechanical Engineers: Tampa, FL, USA, 2017; Volume 58370, p. V04AT05A023.
7. Copaci, D.; Moreno, L.; Blanco, D. Two-Stage Shape Memory Alloy Identification Based on the Hammerstein–Wiener Model. *Front. Robot. AI* **2019**, *6*, 83. [CrossRef] [PubMed]
8. Shelyakov, A.; Sitnikov, N.; Borodako, K.; Koledov, V.; Khabibullina, I.; von Gratowski, S. Design of microgrippers based on amorphous-crystalline TiNiCu alloy with two-way shape memory. *J. Micro-Bio Robot.* **2020**, *16*, 43–51. [CrossRef]
9. Hussain, S.; Pandey, A.; Dasgupta, R. Designed polycrystalline ultra-high ductile boron doped Cu–Al–Ni based shape memory alloy. *Mater. Lett.* **2019**, *240*, 157–160. [CrossRef]
10. Al-Maliki, W.A.K.; Al-Hasnawi, A.G.T.; Wahhab, H.A.A.; Alobaid, F.; Epple, B. A Comparison Study on the Improved Operation Strategy for a Parabolic trough Solar Power Plant in Spain. *Appl. Sci.* **2021**, *11*, 9576. [CrossRef]
11. Álvares da Silva, G.H.; Otubo, J. Designing NiTiAg Shape Memory Alloys by Vacuum Arc Remelting: First Practical Insights on Melting and Casting. *Shape Mem. Superelast.* **2018**, *4*, 402–410. [CrossRef]
12. Zeng, Z.; Oliveira, J.P.; Ao, S.; Zhang, W.; Cui, J.; Yan, S.; Peng, B. Fabrication and characterization of a novel bionic manipulator using a laser processed NiTi shape memory alloy. *Opt. Laser Technol.* **2020**, *122*, 105876. [CrossRef]
13. Khalil-Allafi, J.; Dlouhy, A.; Eggeler, G. Ni_4Ti_3-precipitation during aging of NiTi shape memory alloys and its influence on martensitic phase transformations. *Acta. Mater.* **2002**, *50*, 793. [CrossRef]
14. Zheng, Y.; Zhang, B.; Wang, B.; Wang, Y.; Li, L.; Yang, Q.; Cui, L. Introduction of antibacterial function into biomedical TiNi shape memory alloy by the addition of element Ag. *Acta. Biomater.* **2011**, *7*, 2758–2767. [CrossRef]
15. Baigonakova, G.; Marchenko, E.; Chekalkin, T.; Kang, J.-H.; Weiss, S.; Obrosov, A. Influence of Silver Addition on Structure, Martensite Transformations and Mechanical Properties of TiNi–Ag Alloy Wires for Biomedical Application. *Materials* **2020**, *13*, 4721. [CrossRef] [PubMed]